ACS Sustainable Chemistry & Engineering

Research Article

pubs.acs.org/journal/ascecg

Heat Treatment of Carbonized Hemoglobin with Ammonia for Enhancement of Pore Development and Oxygen Reduction Activity

Jun Maruyama,*[,†] Takahiro Hasegawa,[†] Satoshi Iwasaki,[†] Hidetsugu Kanda,[‡] and Hiroshi Kishimoto[‡]

[†]Environmental Technology Research Division, Osaka Municipal Technical Research Institute, 1-6-50, Morinomiya, Joto-ku, Osaka 536-8553, Japan

[‡]Research & Development Center, Dai Nippon Printing Co., Ltd., 10, Kamikeibucho, Uzumasa, Ukyo-ku, Kyoto 616-8533, Japan

Supporting Information

ABSTRACT: A highly porous carbonaceous material was formed from hemoglobin, which is a natural compound that could be abundantly and inexpensively obtained. Porous carbonized hemoglobin was formed using MgO nanoparticles as a template; in addition, heat treatment of the carbonized hemoglobin with ammonia was performed. Two series of ammonia treatments were examined: long-time heat treatments at various temperatures and high-temperature heat treatments for various times. The specific surface area and, in particular, the pore volume were increased by the ammonia treatment most efficiently at a high temperature for a short period of time. X-ray photoelectron spectroscopy showed a significant decrease in the surface nitrogen concentration and a slight decrease in the surface Fe concentration by the ammonia treatment. The extended X-ray absorption fine structure at the Fe *K*-edge indicated that Fe was coordinated with four nitrogen atoms ($Fe-N_4$ moiety) in the ammonia-treated carbonized hemoglobin. The oxygen reduction activity was evaluated using rotating disk electrodes. The enhancement was observed in accordance with the pore development. A polymer electrolyte fuel cell formed using the ammonia-treated carbonized hemoglobin in the cathode showed an improved performance compared to that formed using the carbonized hemoglobin before the treatment.

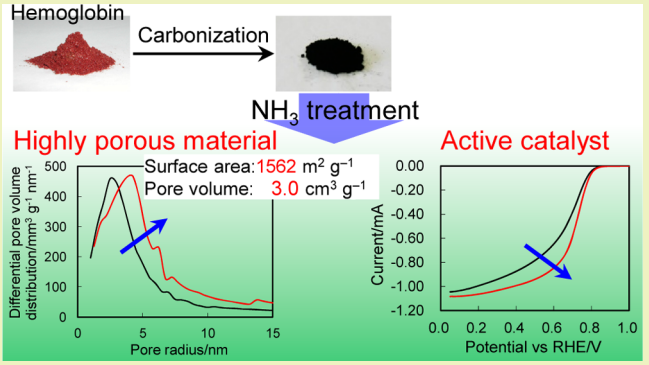

KEYWORDS: *Hemoglobin, Carbonization, Ammonia, Heat treatment, Pore volume, Specific surface area, Electrode catalyst, Oxygen reduction*

INTRODUCTION

Porous carbon materials are classified as one of the major forms of carbon, which are used in many fields, such as catalysts, catalyst supports, gas storage materials, adsorbents, electrodes of electric double layer capacitor, etc. The most typical example is activated carbon, which possesses a high specific surface area of about 1000 $m^2\ g^{-1}$ with a pore volume of about 0.5 $cm^3\ g^{-1}$.[1] Extremely high specific surface areas over 3000 $m^2\ g^{-1}$ for carbon materials formed by, for example, KOH activation and the zeolite template method have been achieved.[2] Quite recently, a carbon material formed from metal−organic frameworks (MOF) has been reported to possess the highest specific surface area and pore volume of 5500 $m^2\ g^{-1}$ and 4.3 $cm^3\ g^{-1}$, respectively.[3] These methods demand, however, special requirements, i.e., expensive vessels like Ni crucibles resistant to corrosive KOH for KOH activation and highly toxic HF to remove the template and metal species for the zeolite template and MOF methods, which lead to high production costs.

Our previous studies have shown the formation of porous carbon materials from proteins, such as catalase and hemoglobin, functioning as a catalyst in the cathode of a polymer electrolyte fuel cell (PEFC).[4−7] The PEFC is a clean and efficient new energy system and is expected to improve the global environment by its widespread use after realization of the active and stable noble metal-free catalysts free from cost inflation and resource limitations. The performances of the PEFCs with the latest carbon-based catalysts are approaching that of the conventional Pt-based PEFC, showing a high potential of the noble metal-free catalysts, although most of them are prepared using expensive or fossil fuel-based and artificially synthesized raw materials.[8−25] In contrast, hemoglobin is one of the materials meeting these requirements based on its abundance and low cost. Hemoglobin could be abundantly obtained, especially from the meat industry that discards hemoglobin-containing blood as waste. Because meat production has increased by 25% in the past decade and reached 250 million tons per year around the world[26] (roughly corresponding to 2.5 million tons per year in hemoglobin), the significance

Received: October 4, 2013
Revised: November 29, 2013
Published: December 3, 2013

of utilizing the waste as functional materials has been increasing also.

Recently, pore development in carbonized hemoglobin and activity enhancement were attained using MgO nanopartcles as a template, which was concurrently generated during carbonization from Mg acetate.[27] Significant advantages of the MgO template method are ease of preparation of the carbon template composite (mixing of the starting materials is possible in solutions and also in powders) and ease of removal of MgO, which is possible even with weak acid solutions like acetic acid.[28] In the present study, the specific surface area and pore volume were further increased by heat treatment of the carbonized hemoglobin with ammonia; the pore volume of 3 $cm^3\ g^{-1}$ obtained under the optimized condition has not been reported before for the carbon materials derived from natural resources to the best of our knowledge. Ammonia and Mg acetate are common and inexpensive compounds, both associated with fertilizers. It has been reported that ammonia treatment enables the pore development of the carbon materials.[29] Two series of ammonia treatments were examined, and the influence of the treatments on pore development, surface concentration of nitrogen and iron, local structure around the iron, and catalytic activity of the oxygen reduction were investigated.

EXPERIMENTAL SECTION

Formation of Carbonized Hemoglobin and Ammonia Treatment. Carbonized hemoglobin was formed by heat treatment of the mixture of hemoglobin and Mg $(CH_3COO)_2$ according to the method described in a previous report[27] and the Supporting Information, which was followed by grinding finely until all of the sample passed a 330 mesh sieve (aperture, 45 μm), a treatment with boiling 2.5 mol dm^{-3} H_2SO_4 for 1 h to remove any soluble Mg and Fe species, washing with high-purity water, and drying in a vacuum at room temperature. The weight ratio of $Mg(CH_3COO)_2$/hemoglobin in the mixture was 3.

The two series of ammonia treatments were (A) long-time heat treatments at various temperatures and (B) high-temperature heat treatments at various times.

Treatment series A: The carbonized hemoglobin was heated in a flowing gas mixture of 50% NH_3 + 50% Ar at 500, 700, 800, 900, and 1000 °C for 3 h after the temperature was raised at 5 °C min^{-1}. The samples obtained at the heat treatment temperatures of T °C (T = 500, 700, 800, 900, 1000) are hereafter labeled as CHbMg-T-3h.

Treatment series B: The carbonized hemoglobin was heated in 50% NH_3 + 50% Ar at 1000 °C for 5, 15, and 30 min after the temperature was increased at 5 °C min^{-1}. The samples obtained by the heat treatment for t min (t = 5, 15, 30) are hereafter labeled as CHbMg-1000-$t$min. The heat treatment that consisted of the temperature increase up to 1000 °C and the immediate temperature decrease without any holding time at 1000 °C was also performed, and the obtained sample is hereafter labeled as CHbMg-1000-0min.

Characterization of Carbonized Hemoglobin Treated with Ammonia. The detailed description is given in previous reports[7,27] and the Supporting Information, and the outline is briefly described below.

The carbonized hemoglobins after the NH_3 treatment, CHbMg-T-3h and CHbMg-1000-$t$min, were characterized by the measurements of the adsorption isotherm of N_2, X-ray photoelectron spectroscopy (XPS), elemental analysis, measurement of the Fe content, and measurement of the extended X-ray absorption fine structures (EXAFS) at the Fe K-edge.

The activity of CHbMg-T-3h and CHbMg-1000-$t$min as the catalysts for the O_2 reduction was evaluated by fixing it on the surface of a rotating glassy carbon disk electrode (GC RDE, geometric surface area of 0.196 cm^2) as a catalyst layer with carbon black as the electron-conductive agent and the perfluorosulfonate ion-exchange resin (Nafion). The addition of carbon black was necessary to improve the electron conduction inside the catalyst layer.[30] The amounts of the catalyst, carbon black, and Nafion on the GC were 60, 60, and 262 μg, respectively. The current–potential relationships for the O_2 reduction were obtained in O_2-saturated 0.1 mol dm^{-3} $HClO_4$ using a Pt wire and a reversible hydrogen electrode (RHE) as the counter and reference electrodes, respectively.

The performance of the PEFC formed using CHbMg-1000-5min for the cathode was measured at 80 °C under atmospheric pressure. The amounts of the catalyst, carbon black, and Nafion in the cathode catalyst layer formed on 5 cm^2 carbon paper treated with polytetrafluoroethylene (ElectroChem) were 3.5, 3.5, and 10 mg cm^{-2}, respectively. The anode was formed on the carbon paper using a commercially available catalyst of 50 wt % platinum on Vulcan XC-72R carbon (Pt/C, Johnson Matthey). The amounts of Pt/C and Nafion in the anode catalyst layer were 1.0 mg cm^{-2} (Pt, 0.5 mg cm^{-2}) and 0.5 mg cm^{-2}, respectively. The electrodes and electrolyte Nafion 112 membrane were pressed at 0.1 MPa and 150 °C for 10 min to form the membrane–electrode assembly, which was then incorporated into a single-cell apparatus (ElectroChem).

RESULTS AND DISCUSSION

Pore Development by Ammonia Treatment. The specific surface areas (S) and pore volumes (V_p) of the carbonized hemoglobin heat treated in 50% NH_3 + 50% Ar are shown in Table 1. In treatment series A, S and V_p increased with an increase in the heat treatment temperature and became nearly constant above 700 °C. These increases were limited to approximately 10% compared to those for the carbonized hemoglobin before the NH_3 treatment. For treatment series B, S and V_p increased with an increase in the heat treatment time up to 5 min and then decreased. An approximate 40% increase in S and 50% increase in V_p were observed. These results indicated that the NH_3 treatment was capable of pore development in the carbonized hemoglobin and that the treatment at high temperature in a short time was effective for pore development. The excessive treatment time would lead to the destruction of the pore structure and decreases in S and V_p.[29]

Table 1. Specific Surface Area (S) and Pore Volume (V_p) of Carbonized Hemoglobin Heat Treated in 50% NH_3 + 50% Ar[a]

	S ($m^2\ g^{-1}$)	V_p ($cm^3\ g^{-1}$)
Before treatment	1110	1.9
Series A		
CHbMg-500-3h	1143	2.0
CHbMg-700-3h	1239	2.3
CHbMg-800-3h	1222	2.2
CHbMg-900-3h	1224	2.2
CHbMg-1000-3h	1192	2.4
Series B		
CHbMg-1000-0min	1270	2.2
CHbMg-1000-5min	1562	3.0
CHbMg-1000-15min	1525	2.7
CHbMg-1000-30min	1312	2.3

[a]Those for carbonized hemoglobin before the treatment are shown for comparison.

Detailed information on the pore development was demonstrated by the pore–volume distribution obtained by using the adsorption isotherm. Figure 1 shows the typical differential pore–volume distributions of the carbonized hemoglobin heat treated with NH_3 by the two treatment series

dx.doi.org/10.1021/sc400402y | ACS Sustainable Chem. Eng. 2014, 2, 493–499

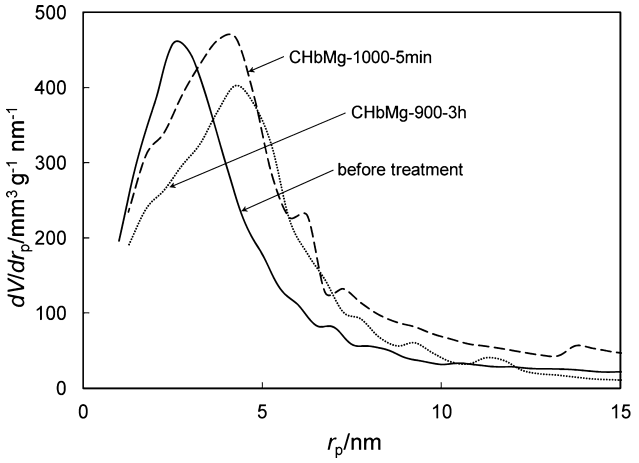

Figure 1. Differential pore−volume distributions of CHbMg-900-3h, CHbMg-1000-5min, and carbonized hemoglobin before NH_3 treatment. V is the pore volume, and r_p is the pore radius.

and before the treatment. Both NH_3 treatments shifted the peak positions to the larger pore radius values. Substantial pore development by treatment series B was also observed in the pore−volume distribution.

Fe and N on Carbonized Hemoglobin Surface. Figure 2a and b show the typical XPS spectra of Fe 2p and N 1s, respectively, for the carbonized hemoglobin heat treated with NH_3 by the two treatment series and before the treatment. The Fe $2p_{3/2}$ binding energies were almost the same for the three kinds of the carbonized hemoglobin. The binding energy of Fe $2p_{3/2}$ was 710.6 eV, indicating that the surface Fe oxidation states was predominantly III, based on the peak positions of the Fe $2p_{3/2}$ binding energy: Fe(III), 710.8−711.8 eV; Fe(II), 707.1−708.7 eV.[31,32] It is possible that at 1000 °C and in NH_3 part of Fe is transformed into iron nitride particles. However, no peak was observed around 706.7 eV corresponding to Fe_xN (x = 2,3,4),[33] indicating the absence of the iron nitride species.

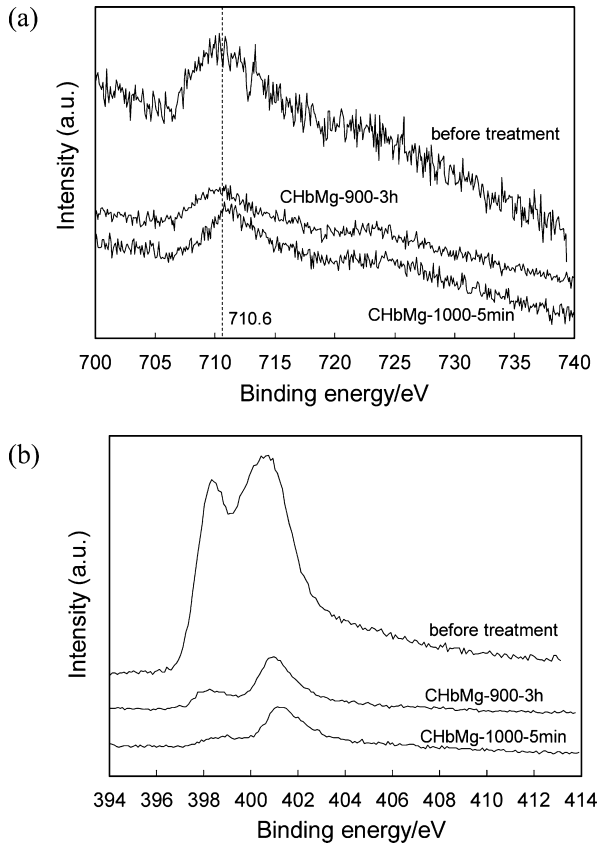

Figure 2. XPS spectra of (a) Fe 2p and (b) N 1s in CHbMg-900-3h, CHbMg-1000-5min, and carbonized hemoglobin before NH_3 treatment. The intensity is normalized by the C 1s intensity.

The N 1s XPS spectra show that the nitrogen atoms were included in the forms of pyridinic- and pyrrolic-type nitrogens, based on the peaks at 398.5 and 400.5−401.0 eV, respectively.[34,35] The intensities were decreased by the NH_3 treatment, particularly for the pyridinic-type nitrogens.

The surface compositions of the carbonized hemoglobin are shown in Table S1 of the Supporting Information. A slight decrease in the surface Fe concentration was observed for the NH_3-treated carbonized hemoglobin. In contrast, the surface N concentration significantly decreased by the NH_3 treatment, as well as the surface O concentration. These XPS results indicated that the NH_3 treatment mainly caused changes in the surface N and O and had a slight influence on the surface Fe. The tendency of the change in the bulk compositions C, N, and O (Table S2, Supporting Information) was similar to that in the surface concentrations. The Fe content was slightly increased by the NH_3 treatment. This slight discrepancy in the tendency between the bulk Fe content and the surface Fe concentration might be due to the higher extent of the carbon exposure by the NH_3 treatment or the loss of surface Fe species during the treatment.

Local Structure Around Fe. Figure 3 shows the RSFs calculated by Fourier transformation of the EXAFS spectra at the Fe K-edge for the carbonized hemoglobin as well as those for hematin and Fe foil for comparison. In the RSF of hematin, the first peak at around 1.7 Å was attributed to four N atoms coordinating to the Fe(III) center. The shoulder at around 1.2 Å was attributed to OH^- coordinating perpendicular to the macrocyclic plane to the Fe center. The second peak at 2.7 Å was attributed to the C atoms, which were bound to the N atom in the pyrrolic ring and the bridging C connecting the pyrrolic rings. The peaks at 1.6 Å in the RSF of the carbonized hemoglobin before the NH_3 treatment, which was similar to the first peaks for hematin, was attributed to the Fe−N_4 moiety derived from protoheme in hemoglobin.[27]

Similar RSFs were also observed for CHbMg-T-3h (T = 500, 700, 800, 900), although the amplitude of the first peak was lower than the carbonized hemoglobin before the NH_3 treatment. The curve fitting analysis was performed to calculate the coordination number of N to Fe (N) and the Fe−N distance (R_{Fe-N}) as well as the Debye−Waller factor (σ) representing the standard deviation from the average R_{Fe-N}.[36] These values for the typical carbonized hemoglobin and hematin are listed in Table 2. The lower amplitude observed for the NH_3-treated carbonized hemoglobin in series A was attributed to the higher σ than that of the carbonized hemoglobin before the treatment. In the RSF for CHbMg-1000-3h, the peaks seen in the Fe foil around 2.1 and 4.3 Å appeared. These peaks indicated the generation of Fe(0) aggregates according to the RSF for the Fe foil.

The peaks around 1.6 Å observed at the RSFs for CHbMg-1000-$t$min (t = 0, 5, 15) were also attributed to the Fe−N_4 moiety. The amplitude further decreased, and the σ values became higher than those for the NH_3-treated carbonized hemoglobin in series A, which resulted in the relatively high

dx.doi.org/10.1021/sc400402y | ACS Sustainable Chem. Eng. 2014, 2, 493−499

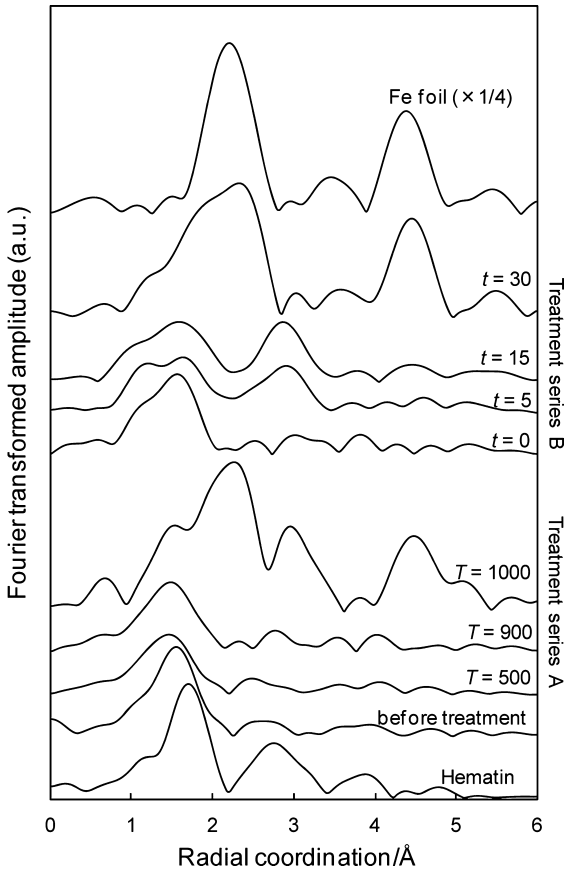

Figure 3. RSFs calculated by Fourier transformation of EXAFS spectra at the Fe *K*-edge for NH_3-treated carbonized hemoglobin in series A and B, carbonized hemoglobin before NH_3 treatment, and Fe foil. The amplitude of the spectrum for the Fe foil is multiplied by 0.25.

Table 2. Number of Nitrogen Coordinated to Fe (N), Distance between Fe and N (R_{Fe-N}), and Debye–Waller Factors (σ) for CHbMg-900-3h, CHbMg-1000-5 min, Hematin, and Carbonized Hemoglobin Before Treatment

	N	R_{Fe-N} (Å)	σ (Å)
hematin	4.0	2.069	0.071
before treatment	4.0	1.980	0.095
CHbMg-900-3h	4.0	1.944	0.109
CHbMg-1000-5min	3.9	2.072	0.121

amplitude of the shoulder around 1.2 Å. The peak appeared around 2.9 Å at the RSFs for t = 5, 15. However, the reason for this is not clear at present, and further studies are necessary. In the RSF for CHbMg-1000-30min, the peaks indicating the generation of the Fe(0) aggregates were also observed around 2.1 and 4.3 Å.

Oxygen Reduction Activity. Figure 4 shows the relationships between the electrode potential and the O_2 reduction currents at the catalyst layers formed using the carbonized hemoglobin heat treated with NH_3 and before the treatment. The current shown in Figure 4 was obtained by subtracting the background current from the measured current. The background current consisted of the currents due to the electrochemical double-layer charging and the redox reaction of the quinone-like surface functional group. The subtraction from the measured current eliminated these influences.

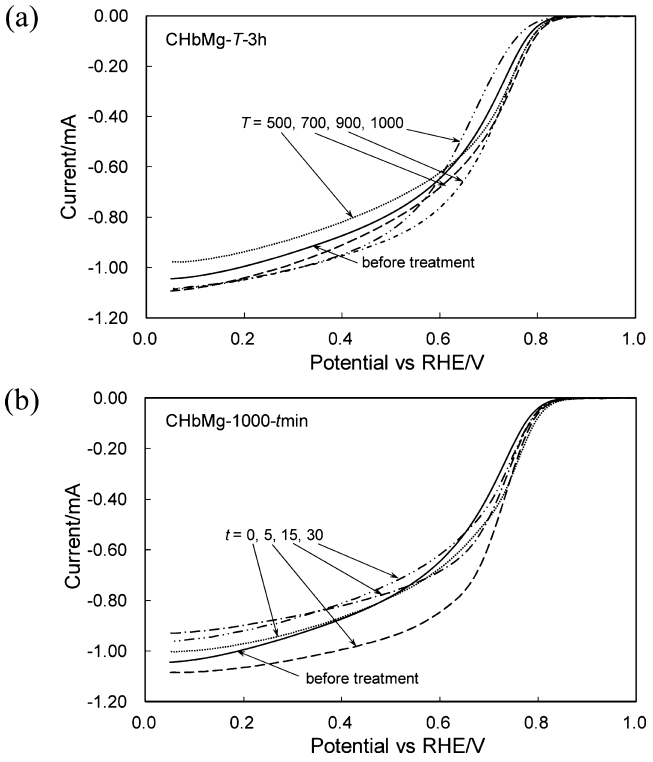

Figure 4. Relationships between electrode potential and oxygen reduction current measured at the rotation speed of 3000 rpm and scan rate of 10 mV s^{-1} in O_2-saturated 0.1 mol dm^{-3} $HClO_4$ at 25 °C for catalyst layers formed from carbonized hemoglobin before NH_3 treatment and NH_3-treated carbonized hemoglobin in series A (a) and B (b).

The O_2 reduction current in the high potential region, typically at 0.7 V, where the influence of the mass transfer in the electrolyte solution and catalyst layer was relatively low, increased with an increase in T in series A up to 700, with similar values from 700 to 900 °C, and then decreased (Figure 5). The current at 0.7 V was chosen based on the assumption that the kinetics could be largely reflected by the current at the potential without any experimental error caused by the low O_2 reduction current at the higher potential.

There is a long controversy over whether the active site is Fe or N on the surface of the carbon materials for the O_2

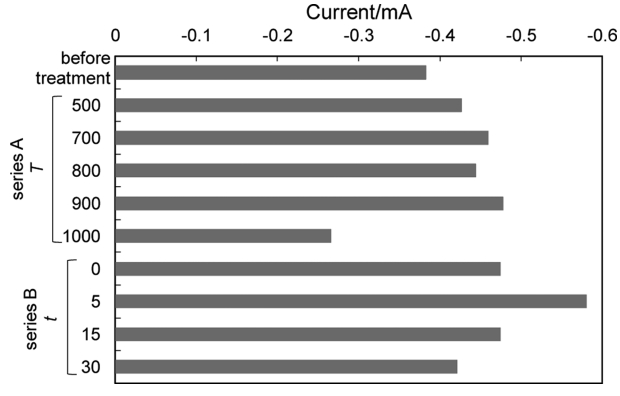

Figure 5. Oxygen reduction current at 0.7 V measured at the rotation speed of 2000 rpm in O_2-saturated 0.1 mol dm^{-3} $HClO_4$ at 25 °C for catalyst layers formed from carbonized hemoglobin before NH_3 treatment and NH_3-treated carbonized hemoglobin.

dx.doi.org/10.1021/sc400402y | ACS Sustainable Chem. Eng. 2014, 2, 493–499

reduction.[37] The XPS results showed that the surface Fe oxidation state was almost the same between CHbMg-900-3h and the carbonized hemoglobin before the NH_3 treatment, indicating the absence of the enhancement effect due to an increase in Fe(II), which is the required species for the first step of the multistep O_2 reduction process.[6,38] The surface Fe concentration only slightly decreased by the NH_3 treatment; however, the surface N concentration was significantly reduced. On the basis of these XPS results and the N_2 adsorption isotherms, it might be reasonable to assume that the active site was the Fe−N_4 moiety at least in the carbonized hemoglobin and that the activity enhancement was attributed to pore development. The activity decrease for CHbMg-1000-3h was attributed to the decomposition of the active site and the generation of Fe(0) aggregates, which was suggested by the EXAFS result.

A similar correlation between the O_2 reduction current and pore development was observed for the NH_3-treated carbonized hemoglobin in series B. The catalyst with the most developed pores obtained in this study (CHbMg-1000-5min) produced the highest O_2 reduction current. The decrease in the O_2 reduction current at the CHbMg-1000-30min catalyst layer compared to the CHbMg-1000-5min and CHbMg-1000-15min catalyst layers was attributed to the lower degree of pore development, decomposition of the active site, and generation of Fe(0) aggregates, which was suggested by the EXAFS result.

Pore development led to an increase in the number of active sites through their exposure on the pore surface from the inside of the carbon matrix.[5,6] Pore development also possessed the effect for enhancing the activity due to the increase in the availability of O_2 molecules for the individual active sites inside the pores in the catalyst. According to a theory proposed by Watanabe et al., there is a potential reaction space around each active site, and the activity will decrease when overlapping of the space occurs by a decrease in the distance between the active site.[39] The increase in the specific surface area could avoid this interference between the active site, and the increase in the pore volume could expand the potential reaction space.

The optimization of the amount of carbon black added in the catalyst layer and the potential applied to the electrode prior to the oxygen current measurement would also enhance the current, which should be examined in future studies.

Fuel Cell Performance. The PEFC was formed using CHbMg-1000-5min that showed the highest O_2 reduction current at 0.7 V in the RDE measurements for the cathode and Pt/C for the anode. The relationships between current density and cell voltage and power density are shown in Figure 6. Compared to the best PEFC formed using the carbonized hemoglobin before the NH_3 treatment (CHbMg3s400900) in our previous study,[27] the current density and maximum power density were higher in spite of the lower amount of the catalyst used in the cathode (3.5 mg cm^{-2}) than in the PEFC cathodes formed using the carbonized hemoglobin in the previous study (5 mg cm^{-2}) (Figures S1 and S2, Supporting Information). Although the performance was lower than that of the PEFC with the latest and highly active noble metal-free cathode catalyst prepared using expensive and artificially synthesized raw materials,[19] the information obtained in this study could be useful in further enhancing the activity of the carbonized hemoglobin, which is derived from one of the abundant renewable natural resources.

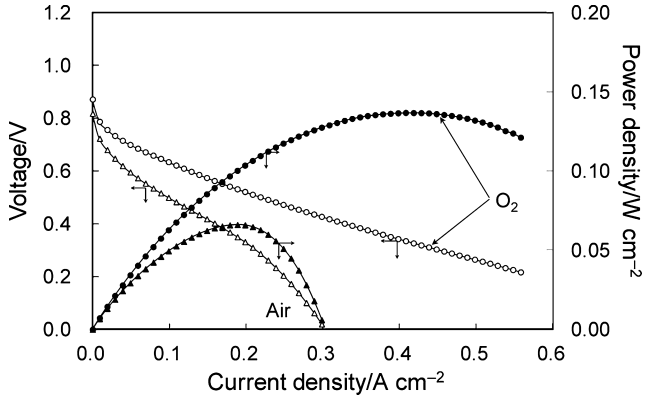

Figure 6. Relationships between current density and cell voltage (white symbols) and relationships between current density and power density (black symbols) for PEFC formed using 3.5 mg cm^{-2} of CHbMg-1000-5min in the cathode and 1 mg cm^{-2} of Pt/C in the anode. Electrode area: 5 cm^2. Cell temperature: 80 °C. Gas humidification temperature: 80 °C. H_2 and O_2 were supplied at 200 cm^3 min^{-1} under atmospheric pressure (circle). H_2 and air were also supplied under atmospheric pressure at 200 and 1000 cm^3 min^{-1}, respectively (triangle).

In addition to the H_2/O_2 measurements, the PEFC performance and its degradation were also examined using H_2/air under atmospheric pressure due to their technological importance. Figure 6 also shows the relationships between the current density, cell voltage, and power density. The current density and maximum power density were slightly higher than those for the PEFC formed using the carbonized hemoglobin in the previous studies. The current decrease during the continuous operation at 0.5 V is shown in Figure S3 of the Supporting Information. The current retained 47% at 100 h, less than that for the PEFC formed using the carbonized hemoglobin before the NH_3 treatment by 16%. Although the detailed reason for the lower durability of CHbMg-1000-5min is not clear at present, it might be associated with the less ordered structure of the Fe−N_4 active site. It is proposed that H_2O_2 generated in the PEFC attacks and decomposes the active site.[40,41] The ordered structure of the Fe−N_4 moiety could be advantageous in avoiding the H_2O_2 attack due to the absence of disordered N, which might be easily attacked. Further studies are necessary to find methods for developing pores with the retention of the ordered structure of the Fe−N_4 moiety.

CONCLUSIONS

Pore development in the carbonized hemoglobin was achieved by heat treatment in the NH_3 + Ar atmosphere at high temperature for a short period of time. The specific surface area and pore volume were increased, and the unprecedented pore volume of 3 cm^3 g^{-1} was obtained for the carbon materials derived from natural resources.

In accordance with pore development, catalytic activity of the carbonized hemoglobin for O_2 reduction was enhanced. The surface N concentration of the carbonized hemoglobin was substantially decreased by the NH_3 treatment, whereas only a slight decrease was observed for the surface Fe concentration. The XAFS measurements showed the presence of the Fe−N_4 moiety in the NH_3-treated carbonized hemoglobin. These results implied that the active site was the Fe−N_4 moiety and that the main factor for the activity enhancement was pore

development. The performance of the PEFC formed using the NH_3-treated carbonized hemoglobin in the cathode was also improved compared to that formed using the carbonized hemoglobin before the treatment.

This study demonstrated that the NH_3 treatment was effective for the formation of highly porous carbonaceous materials with enhanced activity as the fuel cell catalyst from the currently discarded hemoglobin and also implied that the treatment widened the possibility of using hemoglobin as a potential natural resource. Further enhancements of the pore development and catalytic activity would be enabled possibly by more advanced and controlled pore development methods, which are now underway.

■ ASSOCIATED CONTENT

Supporting Information

Experimental details, surface compositions of carbonized hemoglobin, elemental compositions of carbonized hemoglobin, comparison of the fuel cell test results between the present and previous studies.[27] This material is available free of charge via the Internet at http://pubs.acs.org.

■ AUTHOR INFORMATION

Corresponding Author

*E-mail: maruyama@omtri.or.jp. Tel.: +81-6-6963-8043. Fax: +81-6-6963-8049.

Notes

The authors declare no competing financial interest.

■ ACKNOWLEDGMENTS

XAFS measurements were performed with the approval of the SPring-8 (Proposal Nos. 2011B1946 and 2012B1726). We thank Dr. T. Ito for his help with the elemental analysis and Dr. H. Kawano with the ICP-AES measurements.

■ REFERENCES

(1) Maruyama, J.; Sumino, K. -i.; Kawaguchi, M.; Abe, I. Influence of activated carbon pore structure on oxygen reduction at catalyst layers supported on rotating disk electrodes. *Carbon* **2004**, *42*, 3115−3121.

(2) Nishihara, H.; Kyotani, T. Templated nanocarbons for energy storage. *Adv. Mater.* **2012**, *24*, 4473−4498.

(3) Hu, M.; Reboul, J.; Furukawa, S.; Torad, N. L.; Ji, Q.; Srinivasu, P.; Ariga, K.; Kitagawa, S.; Yamauchi, Y. Direct carbonization of Al-based porous coordination polymer for synthesis of nanoporous carbon. *J. Am. Chem. Soc.* **2012**, *134*, 2864−2867.

(4) Maruyama, J.; Abe, I. Formation of platinum-free fuel cell cathode catalyst with highly developed nanospace by carbonizing catalase. *Chem. Mater.* **2005**, *17*, 4660−4667.

(5) Maruyama, J.; Abe, I. Carbonized hemoglobin functioning as a cathode catalyst for polymer electrolyte fuel cells. *Chem. Mater.* **2006**, *18*, 1303−1311.

(6) Maruyama, J.; Okamura, J.; Miyazaki, K.; Abe, I. Two-step carbonization as a method of enhancing catalytic properties of hemoglobin at the fuel cell cathode. *J. Phys. Chem. C* **2007**, *111*, 6597−6600.

(7) Maruyama, J.; Okamura, J.; Miyazaki, K.; Uchimoto, Y.; Abe, I. Hemoglobin pyropolymer used as a precursor of a noble-metal-free fuel cell cathode catalyst. *J. Phys. Chem. C* **2008**, *112*, 2784−2790.

(8) Byon, H. R.; Suntivich, J.; Shao-Horn, Y. Graphene-based non-noble-metal catalysts for oxygen reduction reaction in acid. *Chem. Mater.* **2011**, *23*, 3421−3428.

(9) Masa, J.; Schilling, T.; Bron, M.; Schuhmann, W. Electrochemical synthesis of metal−polypyrrole composites and their activation for electrocatalytic reduction of oxygen by thermal treatment. *Electrochim. Acta* **2012**, *60*, 410−418.

(10) Kannari, N.; Ozaki, J. -i. Formation of uniformly and finely dispersed nanoshells by carbonization of cobalt-coordinated oxine−formaldehyde resin and their electrochemical oxygen reduction activity. *Carbon* **2012**, *50*, 2941−2952.

(11) Kuroki, S.; Hosaka, Y.; Yamauchi, C.; Sonoda, M.; Nabae, Y.; Kakimoto, M. -a.; Miyata, S. Oxygen reduction activity of pyrolyzed polyanilines studied by XPS and ^{15}N solid-state NMR with principal component analysis. *J. Electrochem. Soc.* **2012**, *159*, F309−F315.

(12) Huang, H. -C.; Shown, I.; Chang, S. -T.; Hsu, H. -C.; Du, H. -Y.; Kuo, M. -C.; Wong, K. -T.; Wang, S. -F.; Wang, C. -H.; Chen, L. -C.; Chen, K. -H. Pyrolyzed cobalt corrole as a potential non-precious catalyst for fuel cells. *Adv. Funct. Mater.* **2012**, *22*, 3500−3508.

(13) Kramm, U. I.; Herranz, J.; Larouche, N.; Arruda, T. M.; Lefèvre, M.; Jaouen, F.; Bogdanoff, P.; Fiechter, S.; Abs-Wurmbach, I.; Mukerjee, S.; Dodelet, J. -P. Structure of the catalytic sites in Fe/N/C-catalysts for O_2-reduction in PEM fuel cells. *Phys. Chem. Chem. Phys.* **2012**, *14*, 11673−11688.

(14) Mani, A.; Birss, V. I. Dependence of the oxygen reduction reaction at sol−gel derived Co-based catalysts on acidic solution pH and temperature. *J. Electroanal. Chem.* **2012**, *687*, 102−110.

(15) Zhao, Y.; Watanabe, K.; Hashimoto, K. Self-supporting oxygen reduction electrocatalysts made from a nitrogen-rich network polymer. *J. Am. Chem. Soc.* **2012**, *134*, 19528−19531.

(16) Chisaka, M.; Iijima, T.; Ishihara, Y.; Suzuki, Y.; Inada, R.; Sakurai, Y. Carbon catalyst codoped with boron and nitrogen for oxygen reduction reaction in acid media. *Electrochim. Acta* **2012**, *85*, 399−410.

(17) Zhang, H. -J.; Yuan, X.; Wang, Z.; Yang, J.; Ma, Z. -F. Pyrolyzed iron-triethylenetetramine on carbon as catalyst for oxygen reduction reaction. *Electrochim. Acta* **2013**, *87*, 599−605.

(18) Wu, G.; More, K. L.; Xu, P.; Wang, H. -L.; Ferrandon, M.; Kropf, A. J.; Myers, D. J.; Ma, S.; Johnston, C. M.; Zelenay, P. A carbon-nanotube-supported graphene-rich non-precious metal oxygen reduction catalyst with enhanced performance durability. *Chem. Commun.* **2013**, *49*, 3291−3293.

(19) Tian, J.; Morozan, A.; Sougrati, M. T.; Lefèvre, M.; Chenitz, R.; Dodelet, J.-P.; Jones, D.; Jaouen, F. Optimized Synthesis of Fe/N/C cathode catalysts for PEM fuel cells: A matter of iron−ligand coordination strength. *Angew. Chem., Int. Ed.* **2013**, *52*, 6867−6870.

(20) Leonard, N.; Nallathambi, V.; Barton, S. C. Carbon supports for non-precious metal oxygen reducing catalysts. *J. Electrochem. Soc.* **2013**, *160*, F788−F792.

(21) Yuan, S.; Shui, J. -L.; Grabstanowicz, L.; Chen, C.; Commet, S.; Reprogle, B.; Xu, T.; Yu, L.; Liu, D. -J. A highly active and support-free oxygen reduction catalyst prepared from ultrahigh-surface-area porous polyporphyrin. *Angew. Chem., Int. Ed.* **2013**, *52*, 8349−8353.

(22) Zhang, L.; Kim, J.; Dy, E.; Ban, S.; Tsay, K. -c.; Kawai, H.; Shi, Z.; Zhang, J. Effect of template size on the synthesis of mesoporous carbon spheres and their supported Fe-based ORR electrocatalysts. *Electrochim. Acta* **2013**, *108*, 814−819.

(23) Ramaswamy, N.; Tylus, U.; Jia, Q.; Mukerjee, S. Activity descriptor identification for oxygen reduction on nonprecious electrocatalysts: Linking surface science to coordination chemistry. *J. Am. Chem. Soc.* **2013**, *135*, 15443−15449.

(24) Serov, A.; Robson, M. H.; Smolnik, M.; Atanassov, P. Tri-metallic transition metal−nitrogen−carbon catalysts derived by sacrificial support method synthesis. *Electrochim. Acta* **2013**, *109*, 433−439.

(25) Jiang, R.; Chu, D. Comparative study of $CoFeN_x$/C catalyst obtained by pyrolysis of hemin and cobalt porphyrin for catalytic oxygen reduction in alkaline and acidic electrolytes. *J. Power Sources* **2014**, *245*, 352−361.

(26) Livestock and Poultry: World Markets and Trade. United States Department of Agriculture. http://www.fas.usda.gov/livestock_arc.asp (accessed December 6, 2013).

(27) Maruyama, J.; Hasegawa, T.; Amano, T.; Muramatsu, Y.; Gullikson, E. M.; Orikasa, Y.; Uchimoto, Y. Pore development in carbonized hemoglobin by concurrently generated mgo template for

activity enhancement as fuel cell cathode catalyst. *ACS Appl. Mater. Interfaces* **2011**, *3*, 4837−4843.
(28) Morishita, T.; Soneda, Y.; Tsumura, T.; Inagaki, M. Preparation of porous carbons from thermoplastic precursors and their performance for electric double layer capacitors. *Carbon* **2006**, *44*, 2360−2367.
(29) Proietti, E.; Jaouen, F.; Lefèvre, M.; Larouche, N.; Tian, J.; Herranz, J.; Dodelet, J.-P. Iron-based cathode catalyst with enhanced power density in polymer electrolyte membrane fuel cells. *Nat. Commun.* **2011**, *2*, DOI: 10.1038/ncomms1427.
(30) Maruyama, J.; Abe, I. Application of conventional activated carbon loaded with dispersed Pt to PEFC catalyst layer. *Electrochim. Acta* **2003**, *48*, 1443−1450.
(31) Johansson, L. Y.; Larsson, R.; Blomquist, J.; Cederström, C.; Grapengiesser, S.; Helgeson, U.; Moberg, L. C.; Sundbom, M. X-ray photoelectron and mössbauer spectroscopy on a variety of iron compounds. *Chem. Phys. Lett.* **1974**, *24*, 508−513.
(32) Choudhury, T.; Saied, S. O.; Sullivan, J. L.; Abbot, A. M. Reduction of oxides of iron, cobalt, titanium and niobium by low-energy ion bombardment. *J. Phys. D: Appl. Phys.* **1989**, *22*, 1185−1195.
(33) Biwer, B. M.; Bernasek, S. L. Electron spectroscopic study of the iron surface and its interaction with oxygen and nitrogen. *J. Electron Spectrosc. Relat. Phenom.* **1986**, *40*, 339−351.
(34) Jiménez-Mateos, J. M.; Fierro, J. L. G. X-ray photoelectron spectroscopic study of petroleum cokes. *Surf. Interface Anal.* **1996**, *24*, 223−236.
(35) Casanovas, J.; Ricart, J. M.; Rubio, J.; F. Illas, F.; Jiménez-Mateos, J. M. Origin of the large N 1s binding energy in X-ray photoelectron spectra of calcined carbonaceous materials. *J. Am. Chem. Soc.* **1996**, *118*, 8071−8076.
(36) Bron, M.; Radnik, J.; Fieber-Erdmann, M.; Bogdanoff, P.; Fiechter, S. EXAFS, XPS and electrochemical studies on oxygen reduction catalysts obtained by heat treatment of iron phenanthroline complexes supported on high surface area carbon black. *J. Electroanal. Chem.* **2002**, *535*, 113−119.
(37) Kobayashi, M.; Niwa, H.; Saito, M.; Harada, Y.; Oshima, M.; Ofuchi, H.; Terakura, K.; Ikeda, T.; Koshigoe, Y.; Ozaki, J.-i.; Miyata, S. Indirect contribution of transition metal towards oxygen reduction reaction activity in iron phthalocyanine-based carbon catalysts for polymer electrolyte fuel cells. *Electrochim. Acta* **2012**, *74*, 254−259.
(38) Maruyama, J.; Abe, I. Structure control of a carbon-based noble-metal-free fuel cell cathode catalyst leading to high power output. *Chem. Commun.* **2007**, 2879−2881.
(39) Watanabe, M.; Sei, H.; Stonehart, P. The influence of platinum crystallite size on the electroreduction of oxygen. *J. Electroanal. Chem.* **1989**, *261*, 375−387.
(40) Lefèvre, M.; Dodelet, J.-P. Fe-based catalysts for the reduction of oxygen in polymer electrolyte membrane fuel cell conditions: Determination of the amount of peroxide released during electroreduction and its influence on the stability of the catalysts. *Electrochim. Acta* **2003**, *48*, 2749−2760.
(41) Schulenburg, H.; Svetoslav, S.; Schünemann, V.; Radnik, J.; Dorbandt, I.; Fiechter, S.; Bogdanoff, P.; Tributsch, H. Catalysts for the oxygen reduction from heat-treated iron(III) tetramethoxyphenylporphyrin chloride: structure and stability of active sites. *J. Phys. Chem. B* **2003**, *107*, 9034−9041.